Batteries & Supercaps

Research Article
doi.org/10.1002/batt.202400430

Chemistry Europe
European Chemical Societies Publishing

www.batteries-supercaps.org

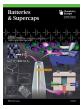

Diffusion Coefficient and Viscosity of Methyl Viologen Electrolyte Estimation Based on a Kinetic Monte Carlo Computational Approach Coupled with the Mean Square Displacement Method

Jia Yu,[a, b] Emmanuel Baudrin,[a, b, c] and Alejandro A. Franco*[a, b, c, d]

Methyl viologen (MV) and its derivatives are emerging as promising candidates within the organic redox flow battery community due to their commendable reversibility and rapid reaction kinetics. However, experimental observations reveal the influence of solute concentration on the diffusion coefficient and the tendency of MV^+ to form dimers or multimers, affecting electrolyte viscosity. Traditional characterization methods may not fully capture these properties. To explore concentration and state of charge effects on diffusion coefficient and viscosity, a kinetic Monte Carlo (kMC) model coupled with mean square displacement analysis is introduced. The kMC model offers a 3D simulation space with expandable periodic boundary conditions, enabling realistic ion movement. The mean square displacement (MSD) algorithm extracts diffusion coefficients, followed by the estimation of the electrolyte viscosity using the Stokes-Einstein equation. Validation with NaCl solutions precedes adaptation to simulate MV^+·diffusion coefficients at 1.5 M with varying states of charge (SoC), aligning with experimental data. Simulation results indicate increased multimerization at higherSoCs. The diffusion coefficient of fully charged MV^+·decreases with electrolyte concentration due to dimer and multimer formation. This modeling approach provides insights into MV^+·behavior, crucial for organic redox flow battery development.

Introduction

The fundamental challenge in the renewable energy field remains the storage of electricity during off-peak hours for subsequent distribution to the power grid during on-peak hours. Among various energy storage devices, Redox Flow Batteries (RFB) stand out as a promising candidate due to their relatively low cost, high-energy efficiency, and ability to decouple power and energy.[1]

As a crucial component of RFB systems, electrolyte takes the stage in their development and optimization. The complexity of the electrolytes brings multiple parameters that can influence the viability of the electrochemical energy storage systems. The necessity for fluidity of the electrolyte mandates keeping viscosity low to minimize pumping losses. On the other hand, increasing the concentration of electroactive species to enhance the energy density would more likely lead to an increase in the viscosity of the electrolyte. Similarly, improving energy density by raising cell potential through the use of non-aqueous solvents brings trade-offs in terms of viscosity, flammability, and cost. Achieving a universally perfect electrolyte solution is still a challenge.

Another critical aspect in the properties of a potential candidate for either the posolyte or negolyte lies in the kinetics of the electrochemical reactions. This factor, exemplified by the studies on vanadium redox flow batteries (VRFBs), significantly impacts the rate performance of the entire system. The complexity arising from numerous potential parameters underlines the need of using computational modeling approaches.

In recent years, Liu *et al.* reported a low-cost aqueous organic RFB (AORFB) utilizing methyl viologen MV for the negolyte and 4-Hydroxy-4-hydroxy-2,2,6,6-tetramethylpiperidin-1-oxylfor the posolyte with a NaCl-based supporting electrolyte.[2] Despite its advantages, such as fast electrode kinetics and eco-friendly aqueous electrolytes, the electrochemical behavior of MV is influenced by side reactions like dimerization and multimerization[3,4] followed by disproportionation,[5] leading to reduced negolyte capacity.

To better investigate electrolyte properties, modeling methods are employed to gain deeper insights into the dynamic behavior of the system. However, most modeling

[a] Dr. J. Yu, Prof. Dr. E. Baudrin, Prof. Dr. A. A. Franco
Laboratoire de Réactivité et Chimie des Solides (LRCS), UMR CNRS 7314, Université de Picardie Jules Verne, Hub de l'Energie, 15 rue Baudelocque, 80039 Amiens Cedex, France

[b] Dr. J. Yu, Prof. Dr. E. Baudrin, Prof. Dr. A. A. Franco
Réseau sur le Stockage Electrochimique de l'Energie (RS2E), FR CNRS 3459, Hub de l'Energie, 15 rue Baudelocque, 80039 Amiens Cedex, France

[c] Prof. Dr. E. Baudrin, Prof. Dr. A. A. Franco
ALISTORE-European Research Institute, FR CNRS 3104, Hub de l'Energie, 15 rue Baudelocque, 80039 Amiens Cedex, France

[d] Prof. Dr. A. A. Franco
Institut Universitaire de France, 103 Boulevard Saint Michel, 75005 Paris, France
E-mail: alejandro.franco@u-picardie.fr

Supporting information for this article is available on the WWW under https://doi.org/10.1002/batt.202400430

studies on RFBs dealt with metal-based redox couples,[6–12] yet very few reports study redox-active organic molecules. At the molecular level, Density Functional Theory (DFT) has been widely applied in screening redox couples due to a reasonable computational cost and adequate accuracy.[13,14] For example, Ding and Yu reported a comparison of electrochemical characteristics between a series of quinone compounds via DFT calculations combined with experiments.[15] Furthermore, Li and Hikihara developed a three-dimensional model of a metal-free quinone-based organic-inorganic RFB to investigate the impact of electrode thickness on cell performance.[10]

In this study, the kinetic Monte Carlo kMC approach, which has been adopted by researchers in other fields, is chosen.[16–18] As a branch of the Monte Carlo method, kMC aims to tackle the dynamic properties of a system in addition to equilibrium characteristics to solve complex problems using randomly generated numbers.[19] It has been widely applied to computational chemistry and materials science during the past few decades due to its outstanding efficiency, simplicity, and versatility.[17,19–21]

There have already been several research studies carried out in the RFB domain and other battery systems with a porous electrode, in which our group applied the kMC approach to simulate the electrode kinetics. For example, we adapted a kMC model coupled with an electrical double-layer model to simulate the electrode kinetics of the MV negolyte in an RFB half-cell.[20] *Shukla and Franco* developed the first kMC model for semi-solid RFB, in which the model considered the volume expansion of silicon particles and the silicon-carbon network.[22] *Thangavel et al.* developed a kMC model targeting the evolution of the carbon/sulfur meso-structure during the discharging process of lithium-sulfur batteries.[23] *Blanquer et al.* reported an investigation on pore size distribution in the cathode of Li–O_2 cells.[24] *Quiroga et al.* developed a kMC algorithm model coupled with continuum approaches and a coarse-grained molecular dynamics model to investigate the electrochemical reactions and membrane degradation in a Proton Exchange Membrane Fuel Cell.[25,26]

This study is dedicated to the development of a novel kMC-Mean Square Displacement (kMC-MSD) model to extract the diffusion coefficient of $MV^{+\cdot}$ from the electrolyte ensemble, which is the first attempt of application of kMC to address this problem, to the knowledge of the authors. Therefore, as the investigation is intended to focus on the diffusion coefficient of the solute ions, the MSD approach is applied on top of the kMC model, which is a common method for extracting diffusion coefficients in MD models.

The following section presents the experimental methodology and measured values of the diffusion coefficient for MV solutions under different SoC concentrations. Moreover, the modeling methodology of the kMC-MSD model is outlined, along with the approach to estimate the viscosity of the electrolyte solution based on the diffusion coefficient extracted from the MSD algorithm. In the Results and Discussion section, we present the validation of the model initially with a NaCl solution, excluding side reaction events. Then, it is adapted to simulate the diffusion coefficient of the target species in the 1.5 M MV solutions with varying SoCs. The simulation results show coherence with experimental results.

Methodology

Experiment

Experimental kinetic parameters can be obtained using different electrochemical techniques:[27] from cyclic voltammetry using the Randles-Ševčík's equation (diffusion coefficient), using linear voltammetry with rotating disc electrodes (RDE) (diffusion coefficient, rate constant) or using impedance spectroscopy.

From cyclic voltammetry experiments, the peak current i_p is proportional to the electroactive species concentration. Through the Randles-Ševčík equation (Eq. 1), the diffusion coefficient D_0 of the reacting species can be calculated from the slope of the plots of the peak current i_p versus the square root of the scan rate v,

$$i_p = 0.4463nFAC\left(\frac{nFvD_0}{RT}\right)^{\frac{1}{2}}, \quad (1)$$

where F is the Faraday constant and A is the surface area of the electrode in cm^2. C is the bulk concentration of the electroactive species in $mol.cm^{-3}$. The number of electrons transferred in the redox reaction is denoted as n. R and T, are the ideal gas constant and the temperature in Kelvin, respectively.

The advantage of the Randles-Ševčík's equation is the independence from the electrolyte viscosity.

Aside from the Randles-Ševčík's equation, another well-applied method for characterizing organic electroactive molecules in half-cells is the Koutecky-Levich analysis carried out with RDE electrode experiments. The Levich equation is expressed as:

$$i_L = 0.62nFAD_0^{\frac{2}{3}}v^{*\,-\frac{1}{6}}C\omega^{\frac{1}{2}}, \quad (2)$$

with i_L the limiting current, v^* the kinematic viscosity, C the bulk concentration, and ω the rotation speed of the electrode. From the Levich plot (limiting current i_L versus the rotation speed $\omega^{\frac{1}{2}}$), the diffusion coefficient D_0 could thus be obtained from the slope.

In the context of the redox-flow community, it is noteworthy that the influence of the diffusion coefficient on concentration or ionic strength is seldom documented. Typically, values are determined using dilute solutions, limiting their applicability for modeling RFBs with molar range electroactive species.

Introduction to the Overall Computational Approach

The computational approach developed in this study mainly contains two parts, the MSD algorithm and the kMC model. The kMC model simulates the random displacement of soluble ions by following an on-lattice approach, like in our previous work,[30] and a MSD algorithm post-processes the trajectory results of each ion simulated in the kMC model.

The computational approach is implemented in Python, by modifying our kMC source code published in GitHub.[36]

Derived from statistical mechanics, MSD is a measure of the deviation of the position of a molecule or ion from a reference position over time and is applied for the estimation of the diffusion

coefficient.[28] The MSD function is defined by the molecule or ion position at time t, $x(t)$, and its initial position, $x(0)$,

$$MSD = |x(t) - x(0)|^2, \quad (3)$$

From the MSD, the diffusion coefficient can be extracted after a long enough simulation time t with:[29]

$$D_{MSD} = \frac{1}{2N}\frac{dMSD}{dt}, \quad (4)$$

where N is the number of dimensions considered in the simulated system. The simulation system in this study is established in a 3-dimensional space to explicitly mimic the displacement of the MV ions. Therefore, $N = 3$.

In an ideal, unbounded simulation environment (based *e.g.* on kMC or Molecular Dynamics), the MSD curve shows an approximately linear trend. This linearity is originated by the unrestricted translational motion of the molecule or ion within the simulation space. Therefore, the diffusion coefficient can be extracted by fitting the slope of the MSD curve. However, practical considerations, such as computational limitations and concentration constraints, necessitate the use of a simulation box with a limited simulation time in this study. Consequently, the diffusion processes are tested within this confined environment, and the diffusion coefficient is extracted from the initial segment of the MSD curve, as elaborated in the subsequent results section.

The simulated MV^+·electrolyte ensemble in this study adopts a classical kMC 'on-lattice' approach under isothermal assumptions, with a basic lattice size of 5 Å chosen to mirror the dimension of solvated MV^+·and MV^{2+} ions. However, given the objective to investigate the influence of ion concentration on both the diffusion coefficient and viscosity while maintaining ions in a Brownian motion state, the aim is to minimize the impact of other charged ions through electrical field distribution. To achieve this, the unit grid size is adjusted by incorporating the Bjerrum length λ_B which is calculated through Eq. 5,

$$\lambda_B = \frac{e^2}{4\pi\varepsilon_0\varepsilon_r k_B T}, \quad (5)$$

where e is the elementary charge. ε_0 and ε_r are the vacuum permittivity and the dielectric constant of the electrolyte, respectively. k_B stands for the Boltzmann constant. The Bjerrum length signifies the threshold distance between two charged ions, where the motion of charged ions is influenced by both thermal energy and electrostatic interaction energy.[30] Therefore, the unit grid size becomes the calculated Bjerrum length. Figure 1 shows the calculated Bjerrum length of NaCl electrolyte under different concentrations, with the electrolyte permittivity extracted from *Peyman et al.*[31]

As it can be seen from Figure 1, the Bjerrum length continuously increases with the concentration reaching 1.6 nm for 4 M NaCl solutions. Therefore, it becomes necessary to adopt a smaller unit grid size to ensure ample space for ions to move within the simulation box, preventing overcrowding and allowing for an accurate representation of Brownian motion dynamics influenced by variations in ion concentration.

The solvated MV^+, MV^{2+}, $(MV)_n^{n+}$, and Cl^- are represented as hard spherical entities on the simulation grid. Except for *MV* dimers or multimers, the specific conformations of each ion have been neglected. The size difference between MV species and chloride ions is not considered in the mesh.

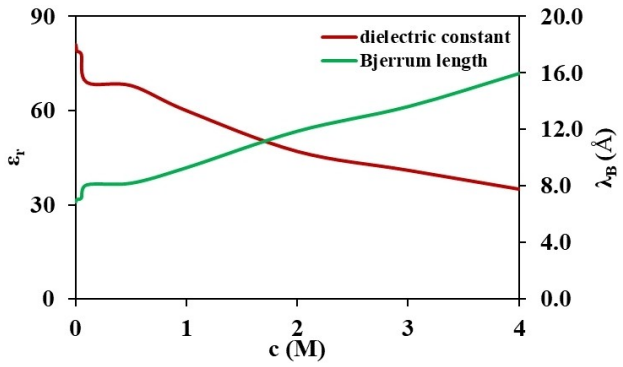

Figure 1. Bjerrum length calculated for NaCl solutions as a function of the salt concentration.

To meet the requirements of the MSD algorithm, an expandable periodic boundary condition is introduced into the kMC model. The expanded boundary condition comprises both periodic boundary conditions and relative expandable boundary conditions. Each movable ion within the simulation box is assigned two sets of coordinates.

The first set is associated with periodic boundary conditions, indicating that if an ion exits the simulation box from the right side, for example, it will reappear at the same position on the left side. Importantly, this set of coordinates does not exceed the dimensions of the simulation box. Simultaneously, a second set of relative expandable boundary condition coordinates is registered for the same ion. This set signifies that if the ion exits the simulation box from any side, the coordinates of the ion will be simply updated based on the step direction.

Taking a simulation box of dimension (5, 5, 5) as an example, if a particle with the coordinate of (4, 5, 1) is moving toward the direction of (0, 1, 0), the periodic boundary condition-controlled coordinate would be (4, 0, 1), while the real position of the trajectory would be (4, 6, 1).

The periodic boundary condition coordinates could then be used to monitor the relative positions of ions, preventing overlaps within the simulation box. Additionally, the coordinates of the relative expandable boundary conditions are utilized to trace the trajectory of the ion and calculate the diffusion coefficient. This dual-coordinate system ensures a robust representation of ion dynamics while addressing potential issues related to the simulation box's boundaries.

kMC Model

The kMC model in this study captures the ion displacement process and traces the trajectories of each ion for the MSD algorithm. The simulated species encompass MV^+, MV^{2+}, Cl^-, and $(MV)_n^{n+}$, where the last signifies the formed MV dimers or multimers.

The workflow of a classic kMC model is depicted in Figure 2. At each iteration, the system configuration undergoes an update, aided by two randomly generated numbers, ρ_1 and ρ_2, which guide the event selection and advance the simulation clock as presented in Figure 2. The real position of each ion is registered in a separate .txt file, which allows the post-processing of the MSD approach. Following the completion of the kMC model, the MSD algorithm is initiated to further analyze the dynamics of ion trajectories.

Research Article
doi.org/10.1002/batt.202400430
Chemistry Europe
European Chemical Societies Publishing

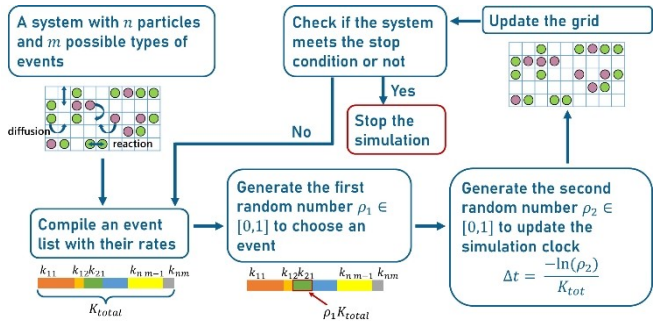

Figure 2. Computational workflow of the kMC model.

The translation event considered in this study is the hopping of ions in six different directions perpendicular to the surface of the cubic mesh with a step size equating to the lattice size. Since the electron transfer process is not included in this study and the unit grid size is already considered through the Bjerrum length, the dominating driving force for the translation is diffusion. The diffusion coefficient of MV^{2+} measured from a dilute electrolyte solution of 1 mM is implemented as the initial diffusion coefficient, $D_0 = 5.86 \times 10^{-6}$ cm^2·s^{-1} (Levich equation) for our computational study. Furthermore, the initial diffusion coefficient for both MV^{+}·and MV^{2+} are considered to be the same.

It is important to clarify here that the initial diffusion coefficient injected in the model does not represent the final diffusion coefficient, D_{MSD}, extracted from the MSD algorithm. D_0 from the most diluted solution is taken as the intrinsic value, which is later impacted by the increase of concentration and the multimerization process.

The translation rate is then calculated through,

$$K_{diff} = \frac{D_{diff}}{A_{diff}}, \tag{6}$$

where A_{diff} is the cross-sectional surface area of the considered species, which depends on the shape and translation direction of the target ion.

It is well reported that dimerization is quite common in MV^{+}·solutions due to the fast kinetics.[3,4] Dimerization was first reported as a side reaction of MV, and then the concept evolved into a multimerization event, which is less discussed.[32] According to Hu *et al.*,[33] the capacity loss of the MV-based negolyte is mainly caused by dimerization followed by disproportionation. In general, the formation of dimers and some trimers has been observed in low-concentration anolytes (0.1 M). At high concentrations of 1 M or higher, it is reasonable to expect the formation of multimers.[34]

While the formation of multimers is infrequently addressed in the literature, the inclusion of multimerization in the kMC model is motivated by the observed significant increase in viscosity along with the SoC from experimental results (as illustrated in Figure 5). Additionally, the exceptionally low energy barrier for dimerization, further suggests the feasibility of subsequent multimerization.[4]

The dimerization/multimerization event is considered in the kMC model when two MV^{+}·are neighbors or a multimer $(MV)_n^{n+}$ is next to an MV^{+}. Then, the product from the multimerization is one multimer occupying all the cubic mesh of both reactants.

The dimerization event occurs at an exceptionally rapid pace, with a kinetic rate of $K_{mm} = 1 \times 10^{13}\ s^{-1}$, which is 10^5 times faster than the translation or rotation events. Indeed, when we convert the measured diffusion coefficient 5.86×10^{-10} m^2.s^{-1} to an event rate in the kMC model, the diffusion coefficient is multiplied by the cross section surface of the ion, which in the simulation is of the order of the nanometer square, which is 10^{-18} m^2. The specific value of the diffusion rate depends on the ion's cross-sectional surface area. Therefore, the diffusion rate ends up in the range of 10^8 s^{-1}. Compared with the dimerization event rate of $K_{mm} = 1 \times 10^{13}\ s^{-1}$, diffusion events (translation ot rotation) are then 10^5 times slower. This suggests that the occurrence of a dimerization event will swiftly dominate the event selection process by the kMC framework. To address this, the dimerization or multimerization events are excluded from the initial kMC event list.

Instead of assembling the event list with significantly varied event rates, the potential for dimerization or multimerization is assessed after each iteration. A random number between 0 and 1 is generated, and if it falls within the range of 0.8–1.0, one of the possible dimerization events will be executed; otherwise, the kMC model proceeds to the next iteration. A multimerization event is only possible when the random number falls between (0.98, 1.0). This approach, optimized through an iterative refinement process to ensure the best compromise between representativeness and computational cost, allows for a balanced consideration of the various events, accounting for the substantial disparities in the event rates (which govern their respective occurrence frequencies).

Compared to the processes of dimerization/multimerization and ion translation, the kinetics for a disproportionation event is relatively slow. The detailed disproportionation rate calculation is discussed in our previous work by Yu *et al.*[20] The difference in terms of magnitude is 10^6, leading to a rare observation of such an event during the simulation. Thus, the disproportionation event is excluded from this study.

In this study, the dimerization and the multimerization of MV^{+} ions, leading to dimers and multimers occupying more than one cubic mesh is included. Therefore, the dimers and multimers with multiple meshes are no longer centrosymmetric as single cubic mesh ions. Thus, the rotation of multimers needs to be taken into account.

The rotation event is considered from the change of conformation of the multimer chain. For each multimer occupying more than one cubic mesh, a specific cube is set to be the base point of the rotation. When a rotation event is chosen, the rest of the cube mesh occupied by the multimer is relocated randomly around the base point, as shown in Figure 3. The sub-molecules of each multimer are labeled by numbers, and the sub-molecule with the number 0 is the base point.

Both rotation and translation are driven by Brownian motion. Thus, the rotation rate is calculated by the same way as for a translation event, while the cross-sectional surface area is related to the entire surface of the considered multimer.

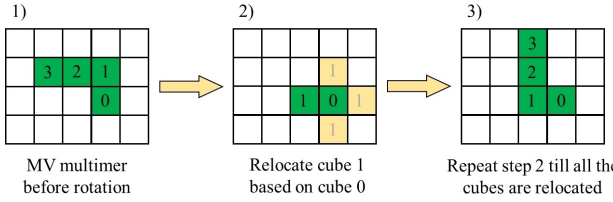

Figure 3. Illustration of the rotation event in the kMC model.

Research Article
doi.org/10.1002/batt.202400430
Chemistry Europe
European Chemical Societies Publishing

Electrolyte Viscosity Estimation

From the Stokes-Einstein equation, the relation between the diffusion coefficient, D_0, of certain species, and the viscosity of the fluid media, η, is described as follows:

$$D_0 = \frac{k_B T}{6\pi\eta r}, \tag{7}$$

In the equation above, r is the radius of the solvation shell. k_B and T are the Boltzmann constant and the temperature, respectively. From this equation, Einstein linked the diffusion coefficient of a 'Stokes' particle undergoing Brownian motion to the dynamic viscosity of a quiescent liquid.[29]

Therefore, by substituting the diffusion coefficient obtained from the MSD algorithm, D_{MSD}, the viscosity of the electrolyte is estimated. Furthermore, considering the multimerization event leads to a change of the components in the solution, only the trajectory of ions without reactions is tracked to estimate the viscosity of the electrolyte (Cl^- *and* MV^{2+}).

Results and Discussion

The refined kMC-MSD model was first tested with NaCl solutions. The concentrations of the simulated NaCl solutions were: 1 mM, 5 mM, 10 mM, 50 mM, 0.1 M, 0.5 M, 1.5 M, and 4 M. The simulation results are presented in Figure 4, with the experimental data ("Ref" in the figure) obtained by Mills.[35] The unit grid size after the consideration of the Bjerrum length and volume limit was set at 6 Å For each concentration, the lattice size was chosen to contain 8 Na^+ ions and 8 Cl^- ions.

The simulation results exhibit trends consistent with the reference experimental data, with improved fidelity to the reference curve at extreme concentrations. However, for concentrations around 0.5 M, the simulation results show some deviations from the experimental reference. Therefore, addressing the outliers and perturbations observed in the intermediate concentration range will be essential for refining the accuracy of the model.

Since the Bjerrum length modified grid size is proved to cope better with experiments in high concentration ranges, the refined kMC-MSD model was then applied to simulate the 1.5 M MV^+·electrolyte under different SoCs, which is defined by the

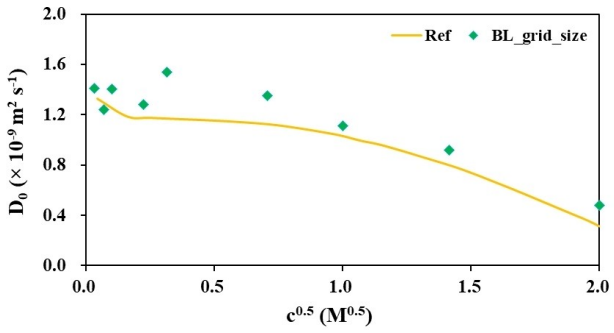

Figure 4. Na^+ diffusion coefficient obtained from the kMC-MSD model with a grid size tuned by the Bjerrum length (green points) and experimental data (Ref, orange curve) by Mills.[35]

percentage of MV^+·in the ensemble, in which 100% MV^+·corresponds to 100% SoC. The extracted diffusion coefficient is then used to estimate the electrolyte viscosity via Eq. 7.

Figure 5c) and d) present the extracted diffusion coefficient and the estimated viscosity from charged MV^+·electrolytes with various concentrations. Compared to the trend of the measured diffusion coefficient of Na^+ presented in Figure 4, the diffusion coefficient of charged MV^+ electrolyte demonstrated a more abrupt decrease along with the increase of concentration, which could be linked to the formation of dimers and multimers as previously discussed.

In the established electrolyte system, the Cl^- ions possess the fastest translation rate. Compared to an MV^+·ion, the translation event rate of a $(MV)_n^{n+}$ ion is at least twice as small, which is dependent on the number n. The bigger the multimers, the more cross-section surface needs to be considered for the translation, leading to a slower translation rate. Therefore, with the increase of SoC, more MV^+·exists in the system, leading to a higher frequency of dimerization and multimerization and a slower translation event rate in the end. Thus, the extracted diffusion coefficient decreases with the increase of SoC.

Figure 5 c) and d) present the extracted diffusion coefficient and the estimated viscosity from charged MV^+·electrolytes with various concentrations. Compared to the trend of the measured diffusion coefficient of Na^+ presented in Figure 4, the diffusion coefficient of charged MV^+ electrolyte demonstrated a more abrupt decrease along with the increase of concentration, which could be linked to the formation of dimers and multimers as previously discussed.

We would like to underline here that the validation of our computational approach is done in two steps. First an experimental diffusion coefficient was obtained from the MV^{2+} solution. However, we lack measurements at different SoCs. We tried to stabilize the SoC in a full cell but we got perturbed by the high reactivity of charged state MV^+ due to the reaction with residual oxygen which did not allow to be sure about the SoC. Due to this, we choose to use data provided by Jena Batteries. We did not get further information from the company about their used experimental conditions which were restricted. However, we feel that based on the two validation steps of our computational approach, the results we obtained and underlined in this work are in quite good agreement with the experimental trends and bringing information to the community which in general consider the diffusion coefficients of both species equal in their modelling works, and independent on their concentration.

The configurations of the simulation box are shown in Figure 6. A video example of the simulation process is provided in the Supporting Information. Due to the expandable periodic boundary conditions, the formed $(MV)_n^{n+}$ are sometimes separated to two opposite sides of the boundaries, explaining the presence of some single pink particles at the edges of the simulation box. In the simulation of 25% SoC, MV dimers dominate the generated $(MV)_n^{n+}$. Along with the increase of SoC, different $(MV)_n^{n+}$ species with $n > 2$ become more predominant in the system, due to the higher population of MV^+.

Research Article
doi.org/10.1002/batt.202400430
Chemistry Europe
European Chemical Societies Publishing

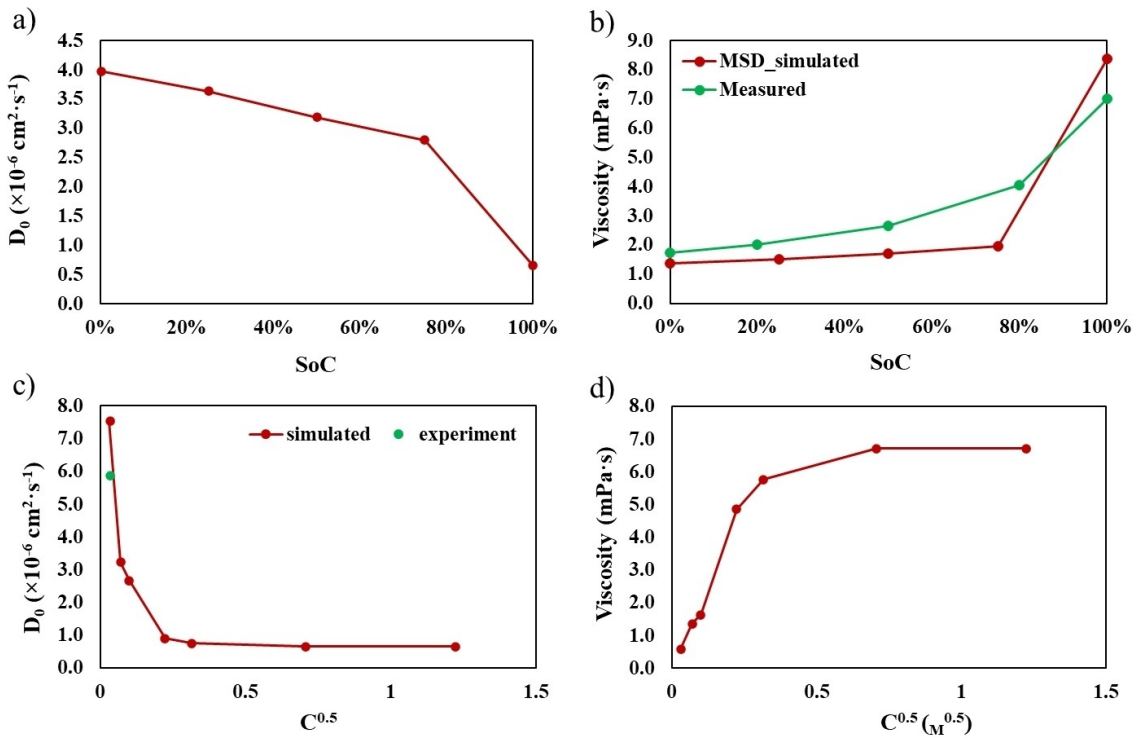

Figure 5. a) Simulated diffusion coefficient of 1.5 M MV electrolyte with different levels of SoC; b) Estimated viscosity of 1.5 M MV electrolyte with different levels of SoC in comparison with experimental results; c) Simulated diffusion coefficient of full charge MV^+ electrolyte with different concentrations; the reference data point is the measured diffusion coefficient of MV^{2+}; d) Estimated viscosity of 1.5 M MV electrolyte with different levels of SoC.

Conclusions and Perspective

This study presents the development of a new computational methodology to assess ionic diffusion coefficients and viscosities of electrolytes used in RFBs. A new kMC model coupled with a MSD approach is reported to study the impact of dimerization and multimerization of MV^+·on its diffusion coefficient and the electrolyte viscosity. This approach, which incorporates a 3D simulation space with expandable periodic boundary conditions, provides a realistic representation of ion movement. Additionally, our study's method of estimating electrolyte viscosity using the Stokes-Einstein equation from diffusion coefficients, validated against NaCl solutions, offers a novel perspective. By aligning simulation results with experimental data and detailing the effects of multimerization on MV^+·diffusion at different states of charge, our research provides critical insights that are essential for optimizing organic RFB performance, marking a significant advancement over traditional characterization methods.

Our kMC model focuses on simulating and tracing the trajectory of target ions under Brownian motion. From the trajectory of each ion, the MSD algorithm analyses the displacement of each ion and extracts the diffusion coefficient. The electrolyte viscosity is estimated based on the extracted diffusion coefficient and the Stokes-Einstein equation.

Three types of event are considered in the kMC model, including the key event of ion displacement under Brownian motion, the dimerization and multimerization process of MV^+·ions, and the rotation of the formed dimers or multimers. The rate of translation and rotation events are calculated from the diffusion coefficient of MV^+·in a diluted system. Due to the very significant difference in terms of rate magnitude, the dimerization and multimerization events are not included in the event list. Instead, another random number is assigned to select the related event. The developed model is first validated by comparison with experimental results of a *NaCl* solution and then applied to simulate a 1.5 M MV electrolyte with different SoCs. The simulated viscosity of the 1.5 M MV^+ anolyte is coherent with the experiment results.

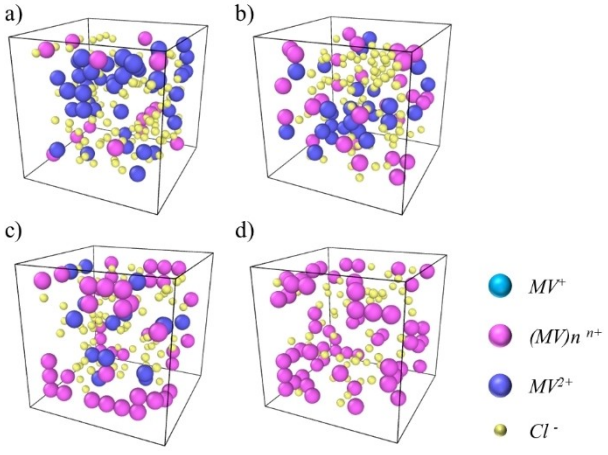

Figure 6. Configuration of the simulation box – 1.5 M MV^- electrolyte. a) SoC = 25 %; b) SoC = 50 %; c) SoC = 75 %; d) SoC = 100 %.

Due to the inherent simplicity of our kMC model, an uncomplicated yet effective approach to simulate the diffusion coefficient and to conduct a preliminary estimation of electrolyte viscosity is reported. Thanks to its simple algorithm workflow, the development of this kMC model can be oriented to simulate other complex events in the future, such as the disproportionation of MV dimers.

Acknowledgements

The authors sincerely acknowledge the funding of the European project SONAR, under Grant Agreement No. 875489. Dr. Noura Rahbani (from Laboratoire de Réactivité et Chimie des Solides, Amiens, France) and Dr. Xian Li (from Jena Batteries) are also acknowledged for providing helpful experimental inputs in the conception of the model. Prof. A. A. Franco acknowledges the Institut Universitaire de France for the support.

Conflict of Interests

The authors declare no conflict of interest.

Data Availability Statement

The data that support the findings of this study are available on reasonable request from the corresponding author.

Keywords: diffusion coefficient · electrolyte viscosity · kinetic Monte Carlo · methyl viologen · organic redox flow battery

[1] M. H. Chakrabarti, R. A. W. Dryfe, E. P. L. Roberts, *Electrochim. Acta* **2007** *52*(5), 2189–2195.
[2] T. Liu, X. Wei, Z. Nie, V. Sprenkle, W. Wang, *Adv. Energy Mater.* **2016**, *6*, 1501449.
[3] M. Wolszczak, Cz. Stradowski, *Radiat. Phys. Chem.* **1989**, *33*(4), 355–359.
[4] L. Naz, M. Mohammad, *J. Chem. Soc. Pak.* **2017**, *39*, 506–515.
[5] D. G. Kwabi, Y. Ji, M. J. Aziz, *Chem. Rev.* **2020**, *120*(14), 6467–6489.
[6] M. Gautam, Z. M. Bhat, A. Raafik, S. Le Vot, M. C. Devendrachari, A. R. Kottaichamy, N. C. Dargily, R. Thimmappa, O. Fontaine, M. O. Thotiyl, *J. Phys. Chem. Lett.* **2012**, *12*, 1374–1383.
[7] D. Zhang, Q. Cai, O. O. Taiwo, V. Yufit, N. P. Brandon, S. Gu, *Electrochim. Acta* **2018**, *283*, 1806–1819.
[8] B. Turker, S. Arroyo Klein, E.-M. Hammer, B. Lenz, L. Komsiyska, *Energy Convers. Manage.* **2013**, *66*, 26–32.
[9] F. Sepehr, S. J. Paddison, *Chem. Phys. Lett.* **2016**, *645*, 20–26.
[10] M. Li, T. Hikihara, *IEICE Transactions on Fundamentals of Electronics, Communications and Computer Sciences* **2008**, *E91(A7)*, 1741–1747.
[11] X. L. Zhou, T. S. Zhao, L. An, Y. K. Zeng, X. H. Yan, *App. Energy* **2015**, *158*, 157–166.
[12] X. Ma, H. Zhang, F. Xing, *Electrochim. Acta.* **2011**, *58*, 238–246.
[13] R. P. Fornari, P. de Silva, *Rev. Comput. Mol. Sci.* Wiley Interdiscip., **2021** *11(2)*, e1495.
[14] N. Rahbani, P. de Silva, E. Baudrin, *ChemSusChem* **2023**, *16*(18), e202300482.
[15] Y. Ding, G. Yu, *Chem* **2017**, *3*(6), 917–919.
[16] Z. Shuai, H. Geng, W. Xu, Y. Liao, J.-M. André, *Chem. Soc. Rev.* **2014**, *43*(8), 2662–2679.
[17] C. Heath Turner, Z. Zhang, L. D. Gelb, B. I. Dunlap, in *Reviews in Computational Chemistry*, Vol. 28, John Wiley & Sons, Ltd, **2015**, pp. 175–204.
[18] R. N. Methekar, P. W. C. Northrop, K. Chen, R. D. Braatz, V. R. Subramanian, *J. Electrochem. Soc.* **2011**, *158*(4), A363.
[19] M. Andersen, C. Panosetti, K. Reuter, *Front. Chem.* **2019**, 7.
[20] J. Yu, G. Shukla, R. P. Fornari, O. Arcelus, A. Shodiev, P. de Silva, A. A. Franco, *Small* **2022**, *18*(43), 2107720.
[21] Y. Yin, C. Gaya, A. Torayev, V. Thangavel, A. A. Franco, *J. Phys. Chem. Lett.* **2016**, *7*(19), 3897–3902.
[22] G. Shukla, A. A. Franco, *J. Phys. Chem. C.* **2018**, *122*(42), 23867–23877.
[23] V. Thangavel, O. X. Guerrero, M. Quiroga, A. M. Mikala, A. Rucci, A. A. Franco, *Energy Storage Mater.* **2020**, *24*, 472–485.
[24] G. Blanquer, Y. Yin, M. A. Quiroga, A. A. Franco, *J. Electrochem. Soc.* **2016**, *163*(3), A329–A337.
[25] M. A. Quiroga, K. Malek, A. A. Franco, *J. Electrochem. Soc.* **2016**, *163*(2), F59–F70.
[26] M. A. Quiroga, A. A. Franco, *J. Electrochem. Soc.* **2015**, *162*(7), E73–E83.
[27] Y. A. Gandomi, D. S. Aaron, J. R. Houser, M. C. Daugherty, J. T. Clement, A. M. Pezeshki, T. Y. Ertugrul, D. P. Moseley, M. M. Mench, *J. Electrochem. Soc.* **2018**, *165*(5), A970.
[28] X. Michalet, *Physical Review E - Statistical, Nonlinear, and Soft Matter Physics* **2010**, *82*(4), 1–13.
[29] P. M. Harman, *English Translation. Albert Einstein, Anna Beck. Isis* **1991**, *82*(4), 768–769.
[30] N. Bjerrum, *Z. Phys. Chem.* **1923**, *106U(1)*, 219–242.
[31] A. Peyman, C. Gabriel, E. Grant, *Bioelectromagnetics* **2007**, *28*(4), 264–274.
[32] S.-I. Imabayashi, N. Kitamura, S. Tazuke, K. Tokuda, *J. Electroanal. Chem. Interfacial Electrochem.* **1988**, *243*(1), 143–160.
[33] B. Hu, Y. Tang, J. Luo, G. Grove, Y. Guo, T. L. Liu, *Chem. Commun.* **2018**, *54*(50), 6871–6874.
[34] Y. Liu, Y. Li, P. Zuo, Q. Chen, G. Tang, P. Sun, Z. Yang, T. Xu, *ChemSusChem.* **2020**, *13*(9), 2245–2249.
[35] R. Mills, *J. Am. Chem. Soc.* **1955**, *77*(23), 6116–6119.
[36] Our kinetic Monte Carlo code that we have used as a basis for the implementation of the computational approach described in this article: https://github.com/ARTISTIC-ERC/SONAR (accessed on December 2024).

Manuscript received: June 28, 2024
Revised manuscript received: December 18, 2024
Accepted manuscript online: December 23, 2024
Version of record online: February 7, 2025